Supporting Information for

A C,S Bonded Quasi-Two-Coordinate Chromium(II) Complex Showing Field-induced Slow Magnetic Relaxation Behaviour

Qian-Cheng Luo,[a] Ning Ge,[a] Yuan-Qi Zhai,[a] Teng-Bo Wang,[b] Lin Sun,*[c] Qi Sun,[d] Fanni Li,[e] Zhongwen Ouyang,[f] Zhen-Xing Wang *[f] and Yan-Zhen Zheng *[a]

1. General Experimental Section

The ligand HSAr* and precursor $CrCl_2(THF)_2$ were synthesized according to the published literature.[1,2] Other reagents were purchased from commercial suppliers without further purification. All manipulations were performed under a dry and oxygen-free argon atmosphere in a glovebox and dehydration and deoxidation treatments were also carried out for all the solvents in solvent purification systems before use.

Syntheses of $Cr(SAr^*)_2$ (1)

HSAr* (257 mg, 0.5 mmol) was dissolved in ether solution (6 mL) under argon atmosphere, then cooled to 0°C in ice water bath. After slowly adding n-BuLi (0.32 mL of a 1.6 M solution in n-hexane) into it, a clear light yellow solution was obtained. The solution was stirred at room temperature for 3 hours and then $CrCl_2(THF)_2$ (67mg, 0.25 mmol) was added. With the mixture stirred for a further 12 hours, the solvents pumped dry and extracted with n-hexane, orange-yellow crystals were isolated through cooling down the filtrate to -35℃ for two days and storing it at room temperature for three days. Yield: 185 mg (68 %). Anal. Calcd (%) for **1**: C, 80.10; H, 9.15; S, 5.94. Found: C, 80.31; H, 9.41; S, 6.06.

2. X-Ray Crystallography Data

All crystal data were collected on a Bruker Apex II DUO area-detector diffractometer with graphite-monochromatic Mo Kα radiation (λ = 0.71073 Å). Cell refinement and data reduction were accomplished with the SAINT processing program. The structures were solved by direct methods and refined on F^2 using Olex 2.[3] CCDC 2128539 (**1**) contains the supplementary crystallographic data for this paper.

Table S1 Crystal data and structure refinement for **1**.

	1
formula	$C_{72}H_{98}CrS_2$
M/g mol^{-1}	1079.62
crystal system	Triclinic
space group	$P\overline{1}$
a, Å	10.431(3)
b, Å	11.687(3)
c, Å	14.658(4)
α, deg	72.627(3)
β, deg	83.920(4)
γ, deg	79.138(4)
V, Å^3	1672.5(8)
Z	1
d_{cal} /g cm^{-3}	1.072
temperature, K	150
θ range	1.458-27.700°
completeness	97%
Goodness-of-fit on F^2	1.023
final indices [$I > 2\sigma(I)$]	$R_1 = 0.0572$, $wR_2 = 0.1652$
R indices (all data)	$R_1 = 0.0833$, $wR_2 = 0.1896$

Table S2 Selected bond lengths (Å) and angle (°) for complex **1**.

Cr-S1	2.352(1)	Cr-S2	2.352(1)
Cr-C1	2.538(2)	Cr-C2	2.538(2)
S1-Cr-C1	81.25(5)	S2-Cr-C2	81.25(5)
S1-Cr-S2	180.0	C1-Cr-C2	180.0

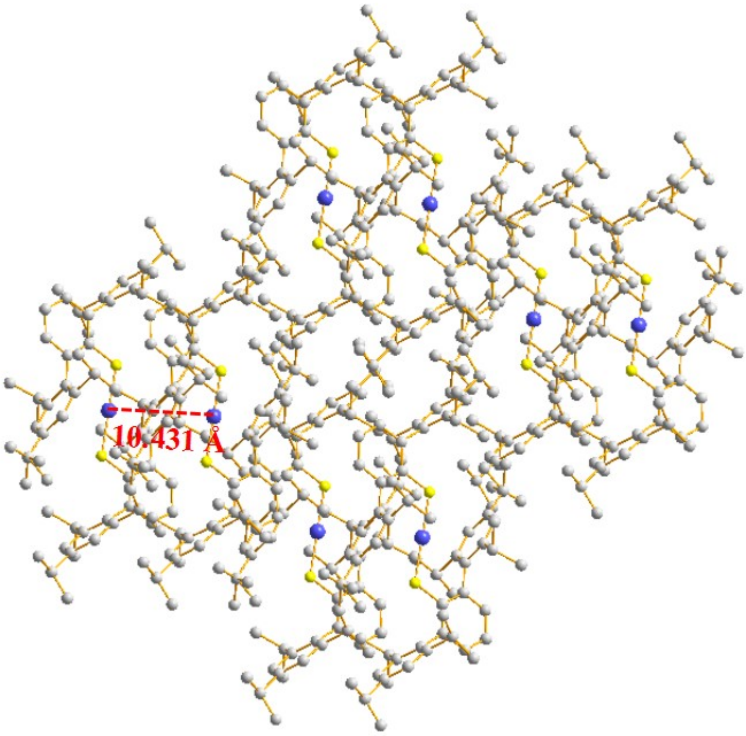

Fig. S1 Packing arrangement of **1**. The dashed lines represent the nearest intermolecular Cr···Cr separation. For clarity, hydrogen atoms are omitted. Colour codes: Cr, purple; S, yellow; C, grey.

3. Magnetic Data

Magnetic measurements were performed using a Quantum Design MPMS-XL7 SQUID magnetometer towards polycrystalline samples which was prepared through mixing with melted eicosane and sealed in polyethylene film. Diamagnetic contributions from the sample holder and the diamagnetism of each sample were considered and estimated using Pascal's constants. All ac magnetic susceptibility data were collected under an oscillating ac field of 3.5 Oe and frequency-dependent ac susceptibility data in the range of 10-1218 Hz were utilized to construct Cole-Cole plots.

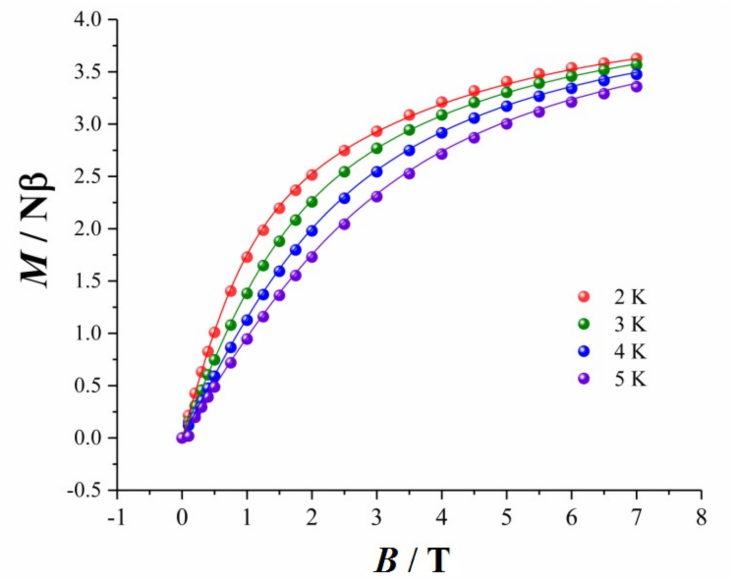

Fig. S2 Field dependent magnetization for **1** at 2-5 K. The solid lines represent the best fit according to the spin Hamiltonian.

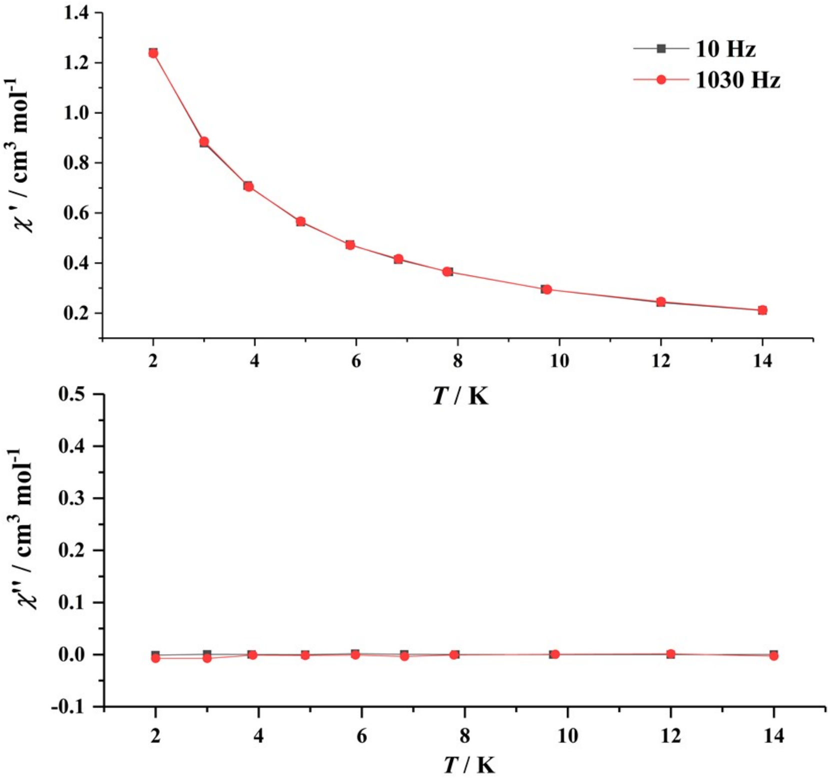

Fig. S3 Temperature dependence of the in-phase (χ') and out-of-phase (χ'') ac susceptibility for **1** under zero dc field. The lines are guides to the eyes.

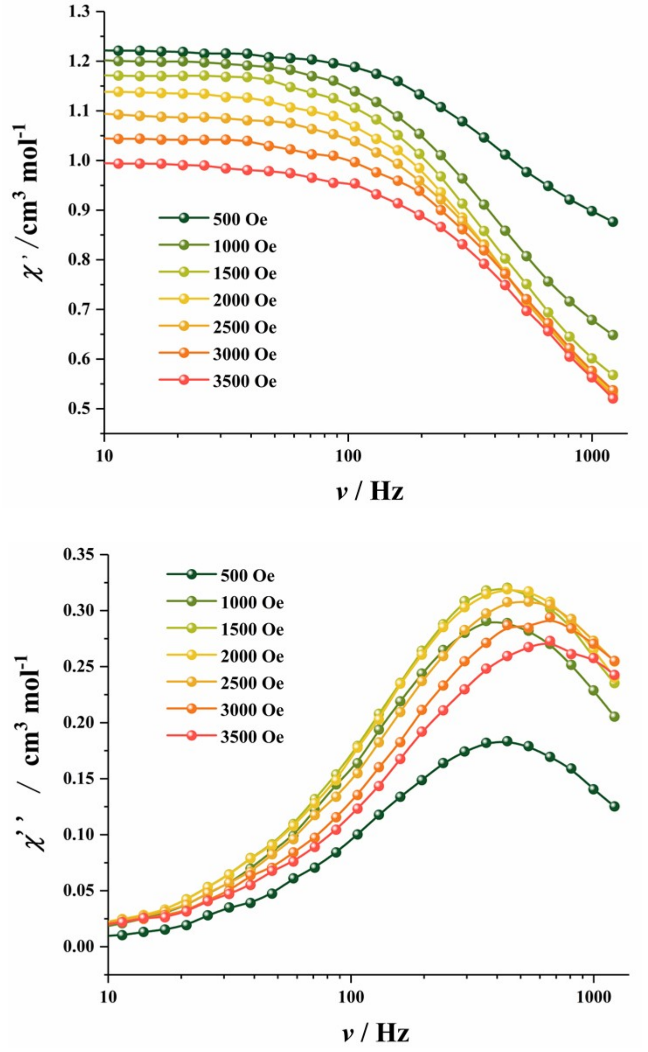

Fig. S4 Frequency dependence of the in-phase (χ') and out-of-phase (χ'') ac susceptibility for **1** at 2 K under different dc fields. The lines are guides to the eyes.

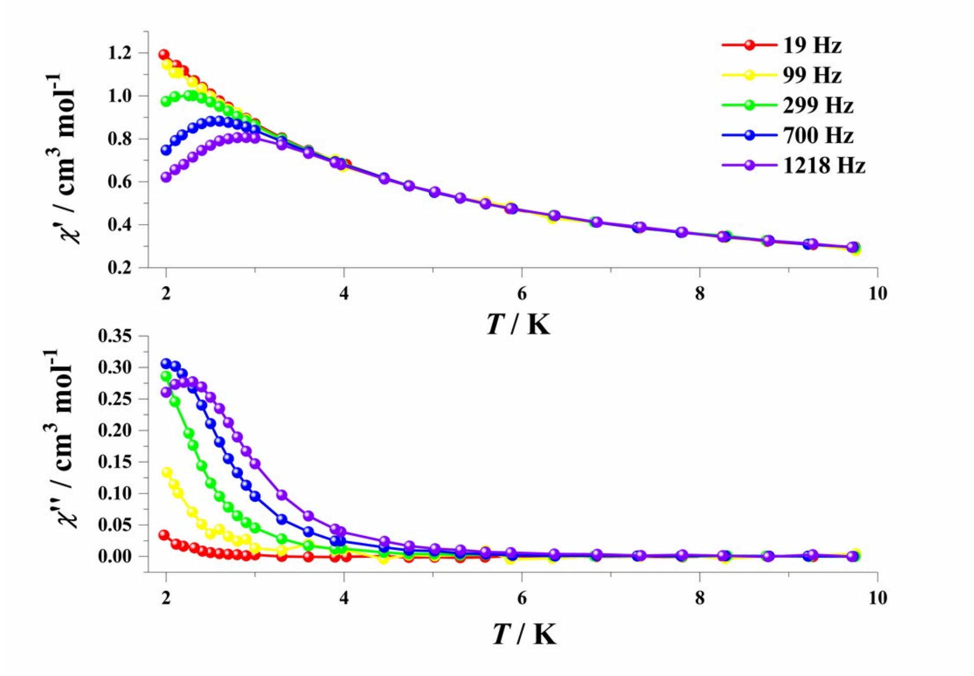

Fig. S5 Temperature dependence of the in-phase (χ') and out-of-phase (χ'') ac susceptibility for **1** under 1500 Oe dc field. The lines are guides to the eyes.

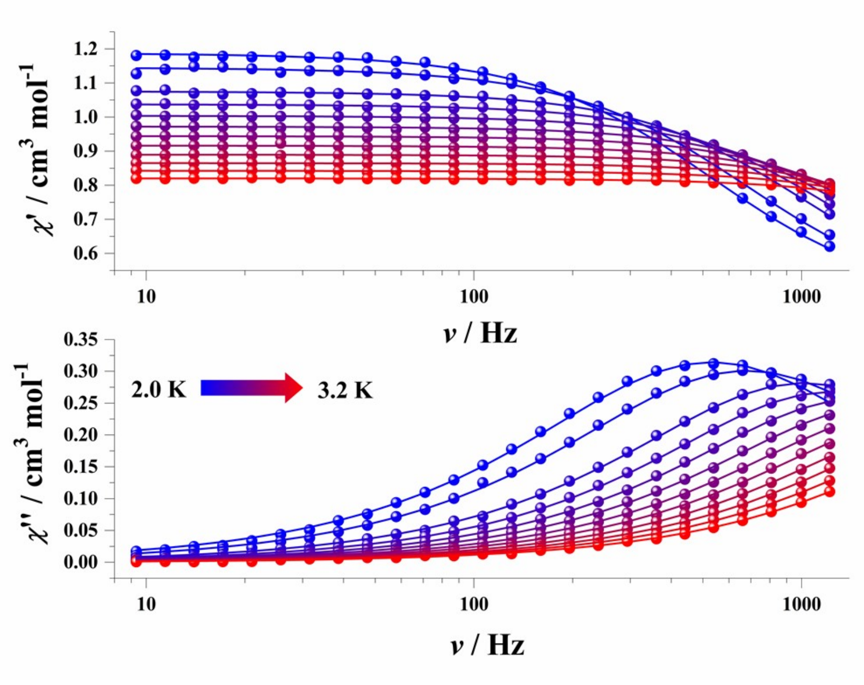

Fig. S6 Frequency dependence of the in-phase χ' (top) and out-of-phase χ'' (bottom) components of the ac susceptibility for **1** measured under 1500 Oe dc field in the temperature range of 2.0-3.2 K. The solid lines represent the fit according to the Cole-Cole results.

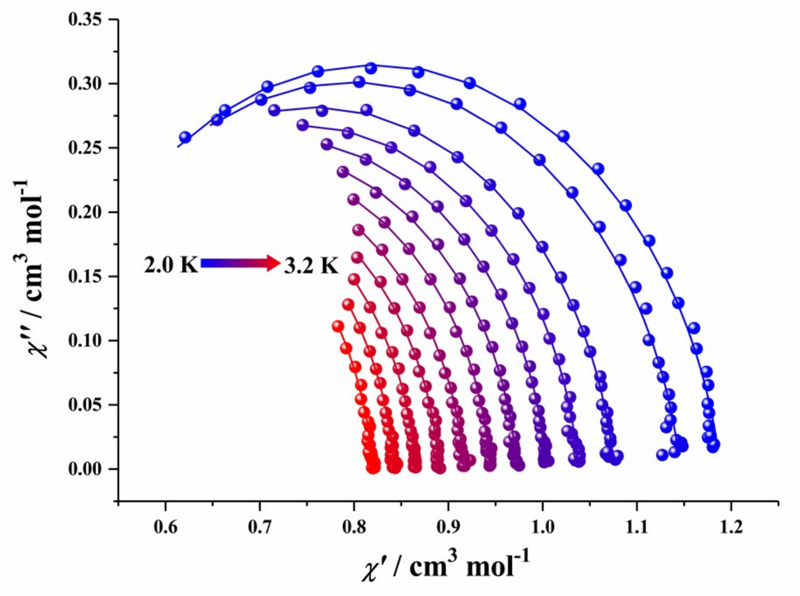

Fig. S7 Cole-Cole plots for **1** at 1500 Oe dc field. The solid lines represent a fit to the data.

Table S3 Relaxation fitting parameters of a generalized Debye model for **1**.

T/*K*	*τ*/*s*	*α*
2.00	2.99E-4	0.10
2.13	2.34E-4	0.09
2.25	1.57E-4	0.08
2.31	1.30E-4	0.07
2.49	1.08E-4	0.06
2.59	8.88E-5	0.06
2.70	7.60E-5	0.06
2.80	6.28E-5	0.06
2.90	5.31E-5	0.05
3.00	4.26E-5	0.06
3.10	3.33E-5	0.06
3.20	2.61E-5	0.07

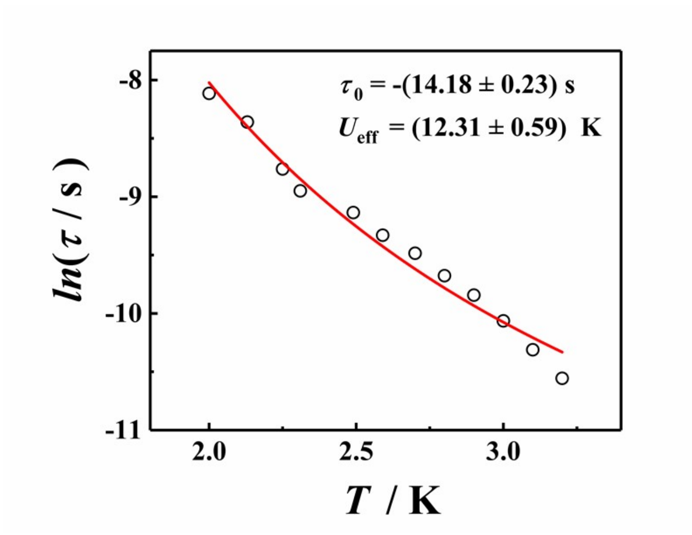

Fig. S8 The relaxation times and corresponding fit for **1** using $\tau^{-1} = \tau_0^{-1} exp(-U_{eff}/k_B T)$.

4. HF-EPR Measurements

HF-EPR measurements were performed on a locally developed spectrometer at Wuhan National High Magnetic Field Centre, using a pulsed magnetic field of up to 30 T at a frequency range from 190 GHz to 405GHz.[4] Then the software SPIN was utilized to simulate experimental spectra and obtain spin Hamiltonian parameters, which developed by Andrew Ozarowski in the National High Magnetic Field Laboratory, USA.

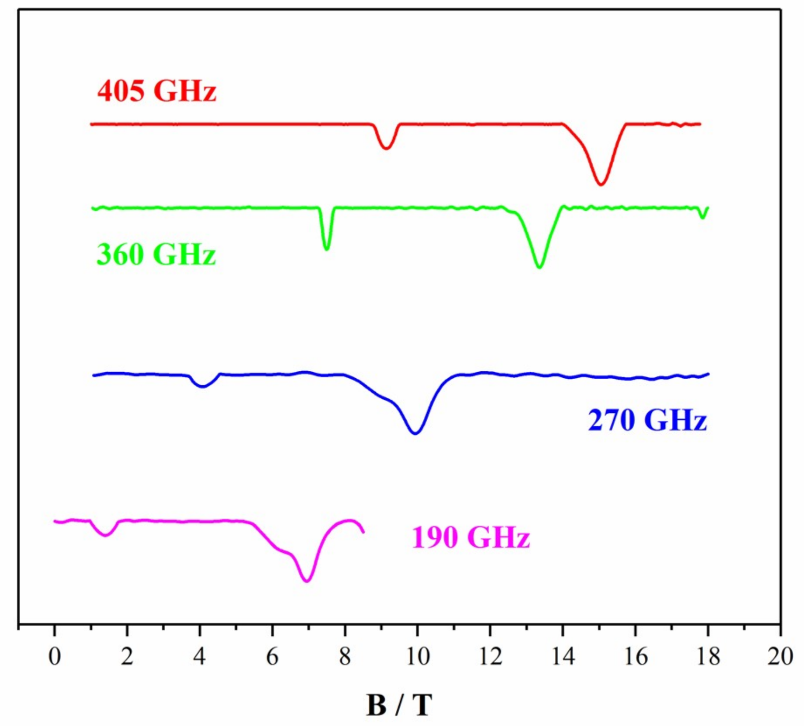

Fig. S9 Variable-frequency EPR spectra collected on a powder sample of **1** at 4.2 K.

5. Electronic Structure Calculations

5.1 *Ab initio* calculations

Ab initio multiconfigurational calculations were performed towards **1** and **2** via ORCA 4.2 package to determine spin Hamiltonian parameters.[5] A standard second order Douglas-Kroll-Hess (DKH2) was considered for scalar relativistic effects for heavy ion chromium(II).[6] The polarized triple-ζ-quality basis set [def2-TZVP] developed by Ahlrichs and co-workers was used for chromium and coordinated sulphur atoms, while the basis set def2-SVP was treated for other remote atoms, such as carbon and hydrogen atoms, as well as corresponding auxiliary basis sets.[7] Dynamic correlation was taken into account by using N-electron valence perturbation theory to second order (NEVPT2) in the state-average (SA)-CASSCF calculations.[8,9] Five 3d orbitals and corresponding four 3d electrons were chosen as active spaces, namely [CAS(4,5)], together with 5 quintets and 35 triplets considered. Tight SCF convergence criteria was adopted and we used RIJCOSX approximation to speed up the calculations and avoid convergence problem.

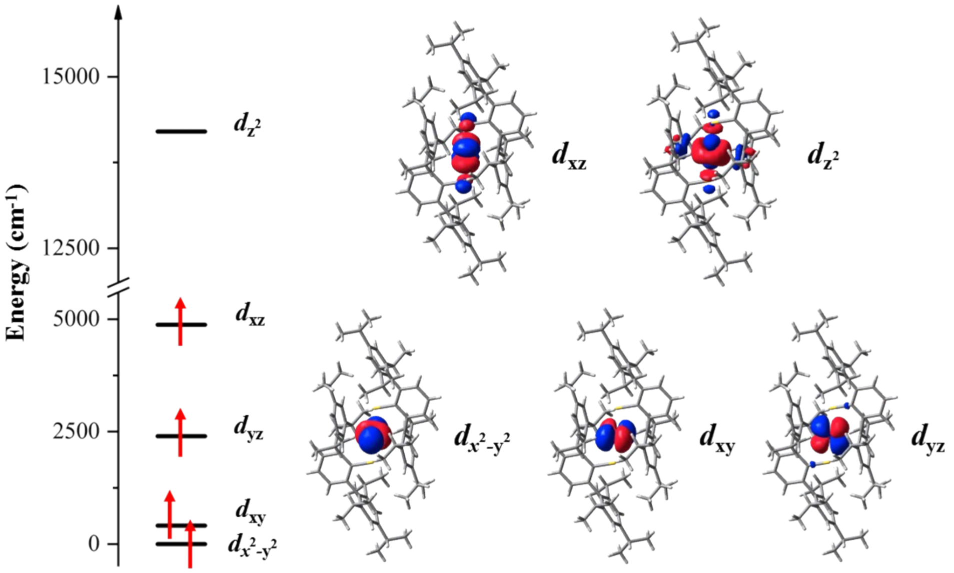

Fig. S10 Calculated active orbital energy orderings for lowest-lying quintet state of complex **1**.

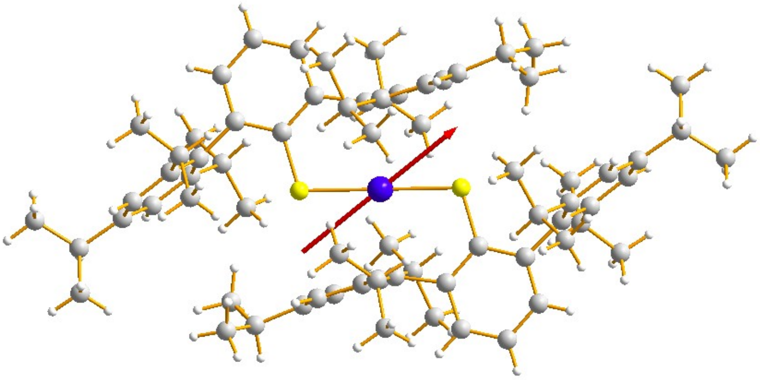

Fig. S11 Calculated orientation of easy axis (red arrow) for complex **1**. Colour codes: Cr, purple; C, gray; S, yellow; H, white.

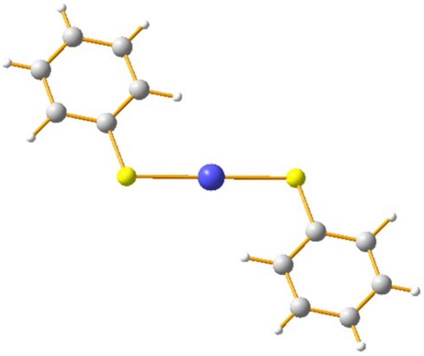

Fig. S12 The structure of model complex **2** (and **3**) used in *ab initio* calculation. Colour codes: Cr, purple; C, gray; S (or O), yellow; H, white.

Table S4 *Ab initio* calculated spin Hamiltonian parameters for **1**.[a]

	1			
	2nd PT-SOC	EHA-SOC	2nd PT-SSC	EHA-SSC
D/cm^{-1}	-1.65	-1.69	-1.65	-2.04
$\lvert E/D \rvert$	0.27	0.27	0.27	0.26
g_x	1.96		1.96	
g_y	1.98		1.98	
g_z	2.00		2.00	
g_{iso}	1.98		1.98	

a. 2nd PT and EHA corresponds to second-order perturbation theory and effective Hamiltonian approach, respectively. “SOC” here represents contribution merely from spin-orbit coupling while “SSC” expresses both contributions of spin-orbit and spin-spin couplings were considered.

Table S5 *Ab initio* calculated spin Hamiltonian parameters for **2**.[b]

	2			
	2nd PT-SOC	EHA-SOC	2nd PT-SSC	EHA-SSC
D/cm^{-1}	-9.55	-9.32	-9.55	-9.54
$\lvert E/D \rvert$	0.14	0.16	0.14	0.17
g_x	1.69		1.69	
g_y	1.93		1.93	
g_z	1.99		1.99	
g_{iso}	1.87		1.87	

b. 2nd PT and EHA corresponds to second-order perturbation theory and effective Hamiltonian approach, respectively. “SOC” here represents contribution merely from spin-orbit coupling while “SSC” expresses both contributions of spin-orbit and spin-spin couplings were considered.

Table S6 The relative energies of *d*-orbitals for for **1** (eV).

1		**2**	
d_{x2-y2}	0	d_{yz}	0
d_{xy}	0.0509	d_{z2}	0.0132
d_{yz}	0.2981	d_{xy}	0.3057
d_{xz}	0.6060	d_{x2-y2}	0.7181
d_{z2}	1.7644	d_{xz}	0.9027

Table S7 Individual contribution to *D*-tensor calculated at CASSCF/NEVPT2 level (cm^{-1}).

Multiplicity	Root	**1**	**2**
5	1	0.297	-9.587
	2	-1.267	0.902
	3	0.074	0.006
	4	-0.013	0.002
3	0	-0.103	-0.123
	1	-0.079	/
	4	-0.176	/
	7	/	0.087
	8	-0.532	/
	10	-0.476	-0.577
	11	/	-0.056
	12	/	0.392
	13	0.180	/
	15	/	0.155
	16	0.205	-0.054
	17	/	-0.121
	21	/	-0.199
	23	/	0.083
	26	0.134	/
	32	/	0.121
	34	0.092	/

Table S8 The relative energies of ground and low-lying quintet spin eigenstates for **1** and **2** (cm^{-1})

	1	**2**
${}^5\psi_0$	0	0
${}^5\psi_1$	7995.1	785.1
${}^5\psi_2$	11085.5	4679.5
${}^5\psi_3$	11831.2	6149.7
${}^5\psi_4$	12220.5	6206.8

5.2 DFT calculations and wave function analysis

To gain stable wave function of complex **1**, the single-point calculation based on Density Function Theory (DFT) was performed using Gaussian 09D.[10] The PBE density functional was employed with Grimme's D3 dispersion correction considered.[11-15] The Stuttgart RSC 1997 effective core potential (ECP) was applied for 10 core electrons of Cr(II) and corresponding valence basis set was used for the remaining valence electrons, while the rest of atoms were treated with cc-pVDZ basis set.[16-19] All converged wave functions are stable under the perturbations considered. To determine chemical bonding characteristics of Cr-S and Cr-C(ipso), Mayer bond order and Atoms in Molecules (AIM) analyses were perfoemed using Multiwfn software.[20]

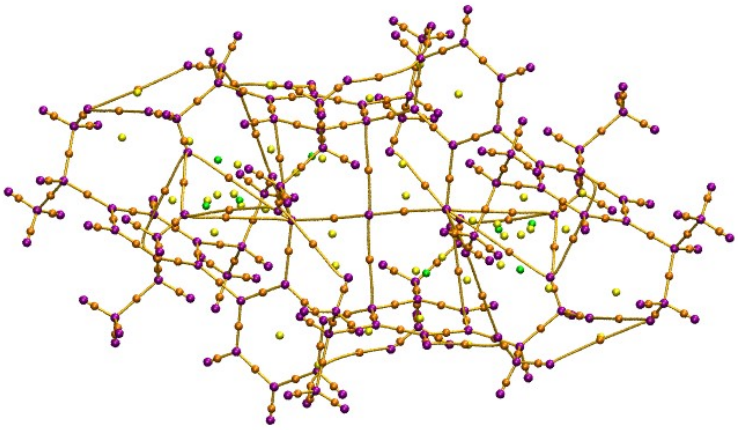

Fig. S13 AIM topology images for **1** containing bond path, (3,-1) points (bond critical points, orange), (3,+1) points (ring critical points, yellow), (3,+3) points (cage critical points, green) as well as (3,-3) points (purple). Poincare-Hopf relationship has been satisfied and all CPs may have been found.

References

1. Schiemenz, B.; Power, P. P. *Organometallics*, **1996**, *15*, 958-964.
2. Kern, R. J. *J. Inorg. Nucl. Chem.*, **1962**, *24*, 1105-1109.
3. Dolomanov, O. V.; Bourhis, L. J.; Gildea, R. J.; Howard, J. A. K.; Puschmann, H. *J. Appl. Cryst.*, **2009**, *42*, 339-341.
4. (a) Wang, S. L.; Li, L.; Ouyang, Z. W.; Xia, Z. C.; Xia, N. M.; Peng, T.; Zhang, K. B. *Acta Phys. Sin.*, **2012**, *61*, 107601; (b) Nojiri, H.; Ouyang, Z. W. *Terahertz Sci. Technol.*, **2012**, *5*, 1.
5. (a) Neese, F. *Wiley Interdiscip. Rev.: Comput. Mol. Sci.*, **2018**, *8*, e1327; (b) Neese, F. *Wiley Interdiscip. Rev.: Comput. Mol. Sci.*, **2012**, *2*, 73–78.
6. Hess, B. A. *Phys. Rev. A: At., Mol., Opt. Phys.*, **1986**, *33*, 3742-3748.
7. (a) Weigend, F.; Ahlrichs, R. *Phys. Chem. Chem. Phys.*, **2005**, *7*, 3297-3305; (b) Schafer, A.; Huber, C.; Ahlrichs, R. *J. Chem. Phys.*, **1994**, *100*, 5829-5835.
8. Roos, B. O. *Ab Initio* Methods in Quantum Chemistry-II, chapter 69, page 399. 1987.
9. Angeli, C.; Cimiraglia, R.; Malrieu, J. P. *J. Chem. Phys.*, **2002**, *117*, 9138-9153.
10. Frisch, M. J.; Trucks, G. W.; Schlegel, H. B.; Scuseria, G. E.; Robb, M. A.; Cheeseman, J. R.; Scalmani, G.; Barone, V.; Mennucci, B.; Petersson, G. A.; Nakatsuji, H.; Caricato, M.; Li, X.; Hratchian, H. P.; Izmaylov, A. F.; Bloino, J.; Zheng, G.; Sonnenberg, J. L.; Hada, M.; Ehara, M.; Toyota, K.; Fukuda, R.; Hasegawa, J.; Ishida, M.; Nakajima, T.; Honda, Y.; Kitao, O.; Nakai, H.; Vreven, T.; Montgomery, J. A., Jr.; Peralta, J. E.; Ogliaro, F.; Bearpark, M.; Heyd, J. J.; Brothers, E.; Kudin, K. N.; Staroverov, V. N.; Kobayashi, R.; Normand, J.; Raghavachari, K.; Rendell, A.; Burant, J. C.; Iyengar, S. S.; Tomasi, J.; Cossi, M.; Rega, N.; Millam, N. J.; Klene, M.; Knox, J. E.; Cross, J. B.; Bakken, V.; Adamo, C.; Jaramillo, J.; Gomperts, R.; Stratmann, R. E.; Yazyev, O.; Austin, A. J.; Cammi, R.; Pomelli, C.; Ochterski, J. W.; Martin, R. L.; Morokuma, K.; Zakrzewski, V. G.; Voth, G. A.; Salvador, P.; Dannenberg, J. J.; Dapprich, S.; Daniels, A. D.; Farkas, Ö.; Foresman, J. B.; Ortiz, J. V.; Cioslowski, J.; Fox, D. J. Gaussian 09; Gaussian, Inc.: Wallingford, CT, 2009.
11. Perdew, J. P., Burke, K., Ernzerhof, M., *Phys. Rev. Lett.,***1996***, 77*, 3865-3868.
12. Perdew, J. P., Burke, K., Ernzerhof, M., *Phys. Rev. Lett.*, **1997**, *78*, 1396-1396; *Phys. Rev. Lett.*, **1996**, *77*, 3865.
13. Grimme, S., *J. Comput. Chem.*, **2004**, *25*, 1463–1473.
14. Grimme, S., *J. Comput. Chem.*, **2006**, *27*, 1787–1799.
15. Grimme, S., *Wiley Interdiscip. Rev. Comput. Mol. Sci.,* **2011**, *1*, 211-228.
16. Giuseppe, L., Ignazio, L. F., *Chem. Phys. Lett.*, **1996**, *255*, 341-346.
17. Lucas, E. A., Stephen, H. Y., George, S. O., Angela, K. W., *J. Chem. Theory Comput.*, **2017**, *13*, 6, 2831-2839.
18. Dunning, T. H., *J. Chem. Phys.,* **1989**, *90*, 1007-1023.
19. Woon, D. E., Dunning, T. H., *J. Chem. Phys.*, **1993**, *98*, 1358-1371.
20. Lu, T.; Chen, F. W. *J. Comput. Chem.*, **2012**, *33*, 580-592.